 CMES, vol.94, no.4, pp.279-300, 2013

The Cell Method: Quadratic Interpolation with Tetrahedra for 3D Scalar Fields

Martino Pani[1], **Fulvia Taddei**[1]

Abstract: The Cell Method (CM) is a numerical method to solve field equations starting from its direct algebraic formulation. For two-dimensional problems it has been demonstrated that using simplicial elements with an affine interpolation, the CM obtains the same fundamental equation of the Finite Element Method (FEM); using the quadratic interpolation functions, the fundamental equation differs depending on how the dual cell is defined. In spite of that, the CM can still provide the same convergence rate obtainable with the FEM. Particularly, adopting a uniform triangulation and basing the dual cells on the Gauss points of the primal edges, the CM is able to reach the 4th order of convergence.
In this note the use of quadratic interpolation to solve the Laplace equation in three-dimensional problems is presented, adopting as primal cell the 10-nodes tetrahedron. A convergence analysis demonstrates that, as in two-dimensional case, the CM with quadratic interpolation can obtain the fourth order of convergence in solving the Laplace equation.

Keywords: Cell Method, Discrete Formulation, Quadratic Interpolation, Laplace Equation

1 Introduction

In the last few years a new purely algebraical formulation of scalar fields (such as thermal conduction, diffusion, electrostatics, acoustics, irrotational fluid flow, etc.) has been developed: the Cell Method (CM). This formulation starts directly from experimental facts and avoids the discretization of the differential equations describing physical laws. This new approach is based on the observation that in every physical theory, the global variables are always referred to geometrical elements of the space such as points, lines, surfaces and volumes.
Due to its adherence with the experimental approach to the physical problem, the CM has been successfully applied in many different fields such as elastostatics

[1] Laboratorio di Tecnologia Medica, Istituto Ortopedico Rizzoli, Bologna.

[Tonti and Zarantonello (2009), Cosmi (2001)], elastodynamics [Tonti and Zarantonello (2010); Cosmi (2005)], electromagnetism [Tonti (2002),Marrone (2001)], acoustics [Tonti (2001a)]. Many technical applications of the CM have been presented in fracture mechanics [Ferretti (2003, 2004b,a, 2005a); Ferretti, Casadio, and Di Leo (2008); Ferretti (2009, 2013a)], fatigue [Cosmi and Hoglievina (2010)], bone mechanics [Cosmi and Dreossi (2007)] and vibrations [Cosmi (2008)]. Furthermore, some direct meshless approach based on the discrete approach of the CM have been proposed [Zovatto and Nicolini (2003, 2007, 2006)] and an application to a technical problem in bone mechanics have been presented [Taddei, Pani, Zovatto, Tonti, and Viceconti (2008)]. Finally, the strict relationship between the algebraic formulation of the CM and the possibility of avoiding spurious solutions in Physics has been shown in Ferretti (2005b) and Ferretti (2013b).

The philosophy of the CM is presented in Tonti (2001b) where the numerical solution of the two-dimensional scalar field is presented using both affine and quadratic interpolation. In that paper it is proved that using simplicial elements with affine interpolation, the CM provides the same fundamental equation produced by the Finite Element Method (FEM); furthermore, it is shown that adopting the quadratic interpolation the CM obtains the fourth convergence order when compared with the theoretical solution of the problem. This order is greater than the value usually obtained by FEM [Zienkiewicz and Taylor (1989)] although FEM shows superconvergence phenomena under specific circumstances [Lin and Zhang (2008); Zhang and Lin (2005); Krizek (2005, 1994, 2005); Babuška, Strouboulis, Upadhyay, and Gangaraj (1996); Brunett (1987); Chen (2006)] mainly related to the regularity of the triangularization and to the kind of discretized equation.

From Tonti (2001b) a question arises: is this convergence rate available also using the CM with quadratic interpolation for three-dimensional problems? In this paper the quadratic formulation of CM for 10-node tetrahedra is presented for the solution of the Laplace equation $\nabla^2 u = 0$. A convergence test over a Dirichlet problem is presented to prove that, in three-dimensional problems as well, the CM can provide the fourth convergence rate value performing as well as the FEM.

2 Quadratic interpolation

2.1 Primal and dual cells

The cell complexes constitute the basis of the discrete approach of the CM. The theoretical bases of the method was widely presented in the works which describe the philosophy of the Method. Nevertheless, it is worth to provide here a brief summary of the key points of the CM. The CM uses global variables associated to the elements of a pair of cell complexes. A cell complex is conceived as a

collection of cells of various dimensions: points (0-cell), edges (1-cell), faces (2-cell) and volumes (3-cell). The primal cell complex is obtained dividing the studied domain (as usually done by the Finite Element Method) by collocating on it a set of points and specifying the topology which define edges, surfaces and contiguous volumes. The dual cell complex is defined from the primal one associating to each primal volume (3-cell) a dual vertex (0-cell). The connection between the dual points produces the elements of the dual cell complex. The duality between the two cell complexes originates form the definition of the dual complex: to each primal volume (0-cell) is associated a dual vertex (0-cell); the primal 1-cells are associated to the dual 2-cells of the primal one, and so on. What is more, the inner orientation established for the cells of the primal complex induces the outer orientation to the cells of the dual complex. The primal cells constitute the natural reference for the configuration variables of the studied field. On the other hand, the dual cell complex offers the reference for the source variables.
The CM calculates the configuration variables at the primal nodes, and uses the dual cells as reference for the balance equation of each primal node. Particularly, the dual volumes constitute the tributary regions which collect the variables involved in the balance equation. The definition of the dual cells starts from the collocation of the dual points associated to the primal volumes. Since no limitations are imposed by the balance equation to the shape and to the extension of the tributary region, the definition of the dual complex is completely arbitrary.
To provide a quadratic interpolation of the configuration variable inside each primal volume a tetrahedron defined by 10 nodes is required; each primal volume is then defined by 4 vertexes and the 6 mid-side points of the edges, as shown in Fig. 1.

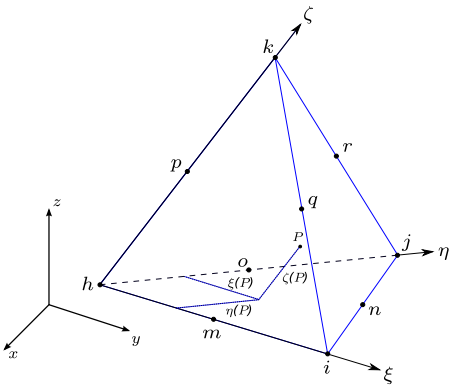

Figure 1: 10-node tetrahedron for the quadratic interpolation: conventional denomination of nodes and local reference system of the affine coordinates.

The dual cell can be obtained dividing each primal volume in parts associated to its nodes; being completely arbitrary, an unique criterion to define the dual cell complex does not exist. Nevertheless, from Tonti (2001b) appears that when the dual subdivision is based on the Gauss points of the primal edges, a higher order of convergence of the solution is obtained. This consideration could constitute a reasonable grounds for basing the dual subdivision of each tetrahedron on the Gauss points of the edges.

The criterion adopted in this study to define the dual cell complex can be summarized as follows:

1. for each primal edge the Gauss points are detected; close to each vertex (e.g. the vertex i) three points (i_1, i_2 and i_3) are defined over the three edges exiting the vertex.

2. for each vertex, the surface based on the three Gauss points close the vertex is defined (e.g. the triangle based on the points i_1, i_2 and i_3); for these triangles, the mid points of the edges as well as the barycentre can be defined (e.g. the mid points i_{12}, i_{23}, i_{31} and the barycentre i_g). These surfaces bound the portions of the primal cell associated to its vertexes. These portions are the part of the dual cells associated to the vertexes which belongs to the primal cell.

3. the barycentre g of the tetrahedron and of its surface (g_h, g_i, g_j and g_k where the subscripts represent the vertex opposite to the considered surface) are detected;

4. for each surface of the tetrahedron, three dual surface are defined: each surface is a quadrilateral obtained connecting the barycentre of the tetrahedron g, the barycentre of the considered surface (e.g. g_h) the mid point of an edge connecting two adjacent Gauss points of the surface (e.g. i_{31}) and the barycentre of the surface associated to this edge (i_g in the example).

This procedure expand inside the volume of the tetrahedron what is done over its surfaces adopting the criterion proposed in Tonti (2001b), as shown in Fig. 2 and Fig. 3.

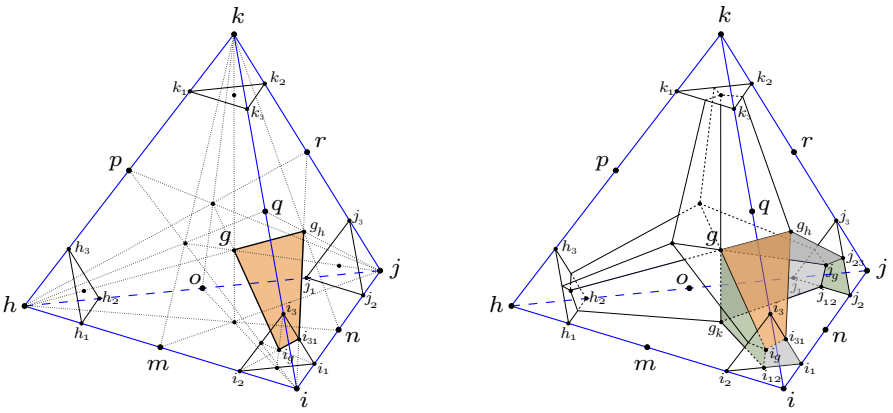

Figure 2: Dual subdivision of a primal cell based on the Gauss points of its edges: the dual portion associated to a vertex is defined by the surface based on the nearest Gauss points of the three edges based on the vertex (considering the vertex h, h_1 h_2 and h_3 are the Gauss points of edges hi, hj and hk, respectively); on the left is highlighted a single piece of the dual surfaces defining the dual cells of the mid-side point n, shown on the right: it is based on the four points g, g_h, i_{31} and i_g; g is the barycentre of the primal cell; g_h is the barycentre of the surface ijk; i_{31} is the midpoint of the segment i_3i_1 based on the gauss points i_1 and i_3 close to the vertex i; i_g is the barycentre of the surface $i_1i_2i_3$ defining the dual portion of the vertex i.

2.2 The local affine coordinates

To interpolate the nodal values of the scalar function onto the primal cell, a quadratic function

$$u_c(x,y,z) = a_1 + a_2x + a_3y + a_4z + a_5xy + a_6yz + a_7zx + a_8x^2 + a_9y^2 + a_{10}z^2 \qquad (1)$$

is used. To deal with a general formulation independently from the single cell geometry a local reference system can be used in each cell, instead of the global Cartesian one. A local reference system is given by the local affine coordinates defined by the 3 edges outgoing a same vertex, as shown in Fig. 1.
The relationship between the local affine and the global Cartesian coordinates is given by:

$$\begin{Bmatrix} x \\ y \\ z \end{Bmatrix} = \begin{Bmatrix} x_h \\ y_h \\ z_h \end{Bmatrix} + \begin{bmatrix} (x_i - x_h) & (x_j - x_h) & (x_k - x_h) \\ (y_i - y_h) & (y_j - y_h) & (y_k - y_h) \\ (z_i - z_h) & (z_j - z_h) & (z_k - z_h) \end{bmatrix} \begin{Bmatrix} \xi \\ \eta \\ \zeta \end{Bmatrix}. \qquad (2)$$

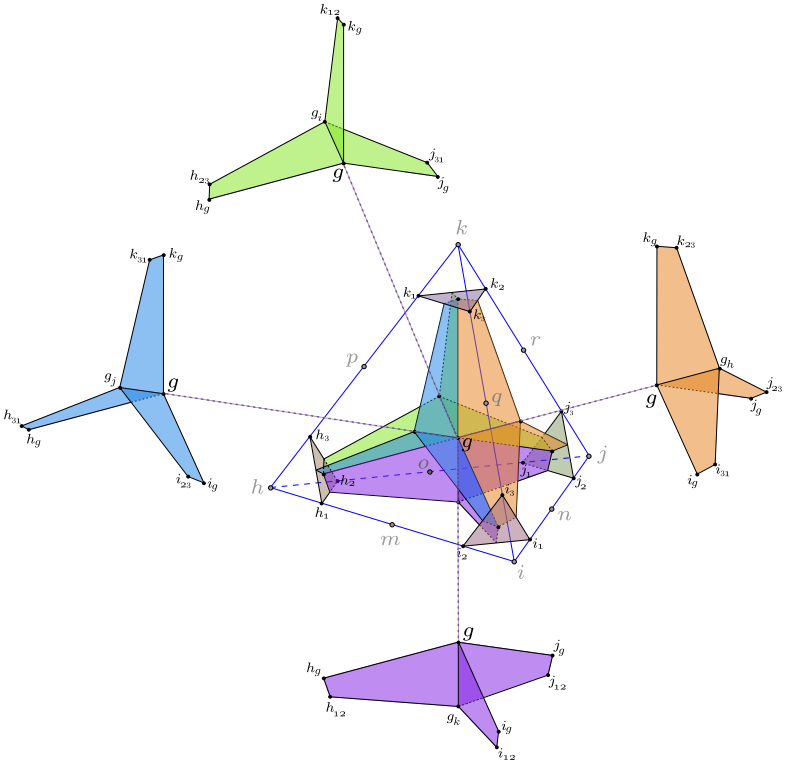

Figure 3: Dual subdivision of a primal cell based on the Gauss points of its edges: exploded view of the dual surfaces associated to the edge nodes with the details of the conventional notation adopted.

The inverse relationship is:

$$\begin{Bmatrix} \xi \\ \eta \\ \zeta \end{Bmatrix} = \begin{Bmatrix} r \\ s \\ t \end{Bmatrix} + \begin{bmatrix} \alpha & \beta & \gamma \\ \delta & \varepsilon & \theta \\ \mu & \nu & \pi \end{bmatrix} \begin{Bmatrix} x \\ y \\ z \end{Bmatrix}. \tag{3}$$

Since the final balance equation does not require any quadrature formula, the adoption of a local reference system is not mandatory. The final balance equation can be formulated by referring all the involved quantities using the global Cartesian coordinates as well. Nevertheless, the positioning of the dual points as well as the availability of a regular shaped tetrahedra to which refer can justify the convenience of a local reference system.

2.3 The interpolating function

The quadratic interpolation of nodal values into the cell c is obtained adopting the second order polynomial function of Eq. 1. On account of the linearity of the relationship between local affine coordinates and the global Cartesian coordinates, the choice of the reference system is absolutely arbitrary. In the local affine reference system the function u_c that interpolate the function $u(x,y,z)$ inside the cell c can be expressed as:

$$u_c(\xi,\eta,\zeta) = \begin{pmatrix} 1 & \xi & \eta & \zeta & \xi\eta & \eta\zeta & \zeta\xi & \xi^2 & \eta^2 & \zeta^2 \end{pmatrix} \begin{Bmatrix} a_h \\ a_i \\ a_j \\ a_k \\ a_m \\ a_n \\ a_o \\ a_p \\ a_q \\ a_r \end{Bmatrix}_c . \tag{4}$$

The 10 coefficients a_y are calculated imposing to the polynomial function to assume the nodal values at the vertices as it follows:

$$\begin{bmatrix} 1 & 0 & 0 & 0 & 0 & 0 & 0 & 0 & 0 & 0 \\ 1 & 1 & 0 & 0 & 0 & 0 & 0 & 1 & 0 & 0 \\ 1 & 0 & 1 & 0 & 0 & 0 & 0 & 0 & 1 & 0 \\ 1 & 0 & 0 & 1 & 0 & 0 & 0 & 0 & 0 & 1 \\ 1 & 1/2 & 0 & 0 & 0 & 0 & 0 & 1/4 & 0 & 0 \\ 1 & 1/2 & 1/2 & 0 & 1/4 & 0 & 0 & 1/4 & 1/4 & 0 \\ 1 & 0 & 1/2 & 0 & 0 & 0 & 0 & 0 & 1/4 & 0 \\ 1 & 0 & 0 & 1/2 & 0 & 0 & 0 & 0 & 0 & 1/4 \\ 1 & 1/2 & 0 & 1/2 & 0 & 0 & 1/4 & 1/4 & 0 & 1/4 \\ 1 & 0 & 1/2 & 1/2 & 0 & 1/4 & 0 & 0 & 1/4 & 1/4 \end{bmatrix} \begin{Bmatrix} a_h \\ a_i \\ a_j \\ a_k \\ a_m \\ a_n \\ a_o \\ a_p \\ a_q \\ a_r \end{Bmatrix}_c = \begin{Bmatrix} u_h \\ u_i \\ u_j \\ u_k \\ u_m \\ u_n \\ u_o \\ u_p \\ u_q \\ u_r \end{Bmatrix}_c \tag{5}$$

inverting this relation the coefficients of the polynome are:

$$\begin{Bmatrix} a_h \\ a_i \\ a_j \\ a_k \\ a_m \\ a_n \\ a_o \\ a_p \\ a_q \\ a_r \end{Bmatrix}_c = \begin{bmatrix} 1 & 0 & 0 & 0 & 0 & 0 & 0 & 0 & 0 & 0 \\ -3 & -1 & 0 & 0 & 4 & 0 & 0 & 0 & 0 & 0 \\ -3 & 0 & -1 & 0 & 0 & 0 & 4 & 0 & 0 & 0 \\ -3 & 0 & 0 & -1 & 0 & 0 & 0 & 4 & 0 & 0 \\ 4 & 0 & 0 & 0 & -4 & 4 & -4 & 0 & 0 & 0 \\ 4 & 0 & 0 & 0 & 0 & 0 & -4 & -4 & 0 & 4 \\ 4 & 0 & 0 & 0 & -4 & 0 & 0 & -4 & 4 & 0 \\ 2 & 2 & 0 & 0 & -4 & 0 & 0 & 0 & 0 & 0 \\ 2 & 0 & 2 & 0 & 0 & 0 & -4 & 0 & 0 & 0 \\ 2 & 0 & 0 & 2 & 0 & 0 & 0 & -4 & 0 & 0 \end{bmatrix} \begin{Bmatrix} u_h \\ u_i \\ u_j \\ u_k \\ u_m \\ u_n \\ u_o \\ u_p \\ u_q \\ u_r \end{Bmatrix}_c \tag{6}$$

or:

$$\mathbf{a}_c = \mathbf{C}\,\mathbf{u}_c. \tag{7}$$

Since local affine coordinates has been adopted, the elements of the matrix $\mathbf{C}$ in Eq. 7 are constant, independent from the cell, its geometry and its spatial collocation. If the global Cartesian coordinates were adopted, these coefficients would be dependent on the coordinates of the cell nodes and the matrix in Eq. 6 would need to be calculated for each cell, causing greater computational cost. If the matrix coefficients would depend on nodal coordinates, the smaller the cell the smaller the values of the matrix coefficients and this might reduce the numerical precision of the calculated inverse matrix, depending on the available computational facilities. Adopting local affine coordinates this problem does not appear, and the precision of the inverse computed matrix is uniform among the cells.
Eq. 4 can be written as:

$$u_c(\xi,\eta,\zeta) = \begin{pmatrix} 1 & \xi & \eta & \zeta\xi\eta & \eta\zeta & \zeta\xi & \xi^2 & \eta^2 & \zeta^2 \end{pmatrix} \mathbf{C}\,\mathbf{u}_c. \tag{8}$$

which express the function's value at point P into the cell c when its local coordinates $\xi\,\eta\,\zeta$ are available.

2.4 Gradient

Inside the generic cell c the gradient vector $\mathbf{g}_c$ is defined as:

$$\begin{Bmatrix} \partial_\xi u \\ \partial_\eta u \\ \partial_\zeta u \end{Bmatrix} = \begin{bmatrix} 0 & 1 & 0 & 0 & \eta & 0 & \zeta & 2\xi & 0 & 0 \\ 0 & 0 & 1 & 0 & \xi & \zeta & 0 & 0 & 2\eta & 0 \\ 0 & 0 & 0 & 1 & 0 & \eta & \xi & 0 & 0 & 2\zeta \end{bmatrix} \mathbf{C}\,\mathbf{u}_c. \tag{9}$$

Its cartesian components are:

$$\begin{Bmatrix} g_x \\ g_y \\ g_z \end{Bmatrix} = \begin{Bmatrix} \partial_x u \\ \partial_y u \\ \partial_z u \end{Bmatrix} = \begin{bmatrix} \partial_x \xi & \partial_x \eta & \partial_x \zeta \\ \partial_y \xi & \partial_y \eta & \partial_y \zeta \\ \partial_z \xi & \partial_z \eta & \partial_z \zeta \end{bmatrix} \begin{Bmatrix} \partial_\xi u \\ \partial_\eta u \\ \partial_\zeta u \end{Bmatrix}. \tag{10}$$

From equation Eq. 3:

$$\begin{Bmatrix} g_x \\ g_y \\ g_z \end{Bmatrix} = \begin{bmatrix} \alpha & \delta & \mu \\ \beta & \varepsilon & \nu \\ \gamma & \theta & \pi \end{bmatrix} \begin{bmatrix} 0 & 1 & 0 & 0 & \eta & 0 & \zeta & 2\xi & 0 & 0 \\ 0 & 0 & 1 & 0 & \xi & \zeta & 0 & 0 & 2\eta & 0 \\ 0 & 0 & 0 & 1 & 0 & \eta & \xi & 0 & 0 & 2\zeta \end{bmatrix} \mathbf{C}\,\mathbf{u}_c. \tag{11}$$

2.5 Constitutive equation

The constitutive equation gives the relationship between the flux density vector **q** and the gradient vector **g** inside each primal volume. For an anisotropic material the constitutive equation assume the form:

$$\begin{Bmatrix} q_x \\ q_y \\ q_z \end{Bmatrix}_c = - \begin{bmatrix} \lambda_{xx} & \lambda_{xy} & \lambda_{xz} \\ \lambda_{yx} & \lambda_{yy} & \lambda_{yz} \\ \lambda_{zx} & \lambda_{zy} & \lambda_{zz} \end{bmatrix}_c \begin{Bmatrix} g_x \\ g_y \\ g_z \end{Bmatrix}_c \tag{12}$$

or, in matricial notation

$$\mathbf{q}_c = -\Lambda_c\, \mathbf{g}_c \tag{13}$$

where Λ_c is a 3x3 matrix. Referring to the heat conduction problem, Eq. 12 is the generalized form of the Fourier equation for a generic anisotropic body and the terms λ_{ij} are the coefficients of thermal conductivity which define the so-called thermal conductivity tensor.
If the material inside the cell c is isotropic Eq. 12 becomes:

$$q_x = -\lambda g_x \qquad q_y = -\lambda g_y \qquad q_z = -\lambda g_z \tag{14}$$

or, in vector form:

$$\mathbf{q}_c = -\lambda\, \mathbf{g}_c. \tag{15}$$

2.6 Flux

Flux is global quantity associated to a surfaces. Inside each primal cell, the gradient vector $\mathbf{g}$ and then the flux density vector $\mathbf{q}$ are affine functions of the nodal coordinates; the total flux Q across the surface A inside a primal cell c can be expressed as the scalar product of two vectors: the area-vector defining the surface and the flux density vector $\mathbf{q}$ evaluated in the surface barycentre G. Denoting by $\mathbf{A} = (A_x, A_y A_z)$ the area-vector and G its barycentre:

$$\Phi(\mathbf{A}) = \mathbf{A}\,\mathbf{q} = \begin{pmatrix} A_x & A_y & A_z \end{pmatrix} \begin{Bmatrix} q_x(G) \\ q_y(G) \\ q_z(G) \end{Bmatrix}. \tag{16}$$

Combining Eq. 16, Eq. 12 and Eq. 11 the flux $Q(A_{n,i})$ can be expressed in terms of nodal unknown values of the prrimal cell where the surface is placed:

$$\Phi(\mathbf{A})_c = \begin{pmatrix} f_h & f_i & f_j & f_k & f_l & f_m & f_n & f_o & f_p & f_q \end{pmatrix}_c \mathbf{u}_c \tag{17}$$

2.7 Fundamental equation

The fundamental equation for a scalar field is obtained writing the balance equation at each primal node. Defined a tributary region associated to each primal node, the flux through its boundary is equivalent to the source rate collected by the tributary region. In the CM the natural tributary regions are offered by the cells of the dual cell complex. Since the structure of the balance equation is independent from both the shape and the extensions of the tributary region, the criterion adopted to define the dual subdivision is arbitrary.

Using the quadratic interpolation with simplicial elements in two-dimensional problems, it has been found that the criterion adopted for the definition of the dual complex could produce effects on the convergence rate of the numerical solution [Tonti (2001b)]. When the dual subdivision is based on the Gauss points of the primal cell edges, the 4th order of convergence was obtained at nodes for the solution of the Laplace equation. On the basis of this fact, the same criterion has been adopted for the dual subdivision of each 10-nodes primal cell, as described in section 2.1.

The fundamental equation is obtained assembling the balance equations referred to each dual cell. There are two ways to do this:

one node at time : considering a primal node n, we will denote by $\Im(n)$ is the set of primal cells sharing the node; this set of cells permit to define the dual cell of the node n. With reference to Fig. 4 and Fig. 5 this dual cell is a polyhedron composed by different parts belonging to the primal cells of $\Im(n)$;

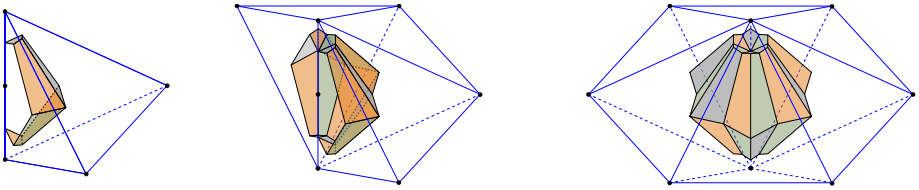

Figure 4: Dual cell of associated to a midside point of the primal cell complex: the figure shows how to merge the dual parts defined in each primal cell with the criterion illustrated in Fig. 2.

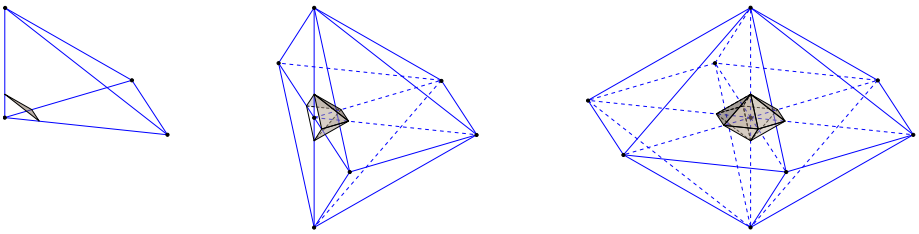

Figure 5: Dual cell associated to a primal vertex: the figure shows how to merge the dual parts defined by the Gauss points of the edges of each primal cell sharing the vertex.

the boundary of the dual cell is composed by polygons $A_{n,i}$ and each polygon belong to a specific primal cell c of $\Im(n)$. To calculate the flux balance it is necessary to calculate the flux $\Phi(A_{n,i})$ crossing each single polygonal surface $A_{n,i}$, inside the corresponding primal cell. Combining Eq. 16, Eq. 12 and Eq. 11 the flux $Q(A_{n,i})$ can be expressed in terms of the unknown function at the nodes of the involved primal cells. Once all flux terms have been calculated, it is possible to write the flux balance on the considered node n, calculating the source terms collected by the dual volume associated to the node:

$$\sum_{c \in \Im(n)} \mathbf{R}^c_{A,i}\, \mathbf{u}_c \;=\; S_h \tag{18}$$

where S_h is the source collected by the dual cell associated to the primal node h and $\mathbf{R}^c_{A,i}$ is the vector of coefficients f_i of Eq. 17. These coefficients express the flux through the area $A_{n,i}$ in terms of the nodal values of the corresponding primal cell c. The resulting equation involves the values of the unknown function at all the nodes of the set $\Im(n)$, and constitutes the row n of the fundamental matrix of the algebraic formulation of the problem.

one cell at time : analysing a single primal cell by time, it is possible to write the fluxes through the contained dual surfaces. These surfaces separate the portions of the primal cell associated to its primal nodes, defining the portions of the dual cells included in the considered primal cell. Combining equations Eq. 11, Eq. 12 and Eq. 16 the flux terms of tributary regions associated to each primal cell node are calculated; the fluxes are expressed in terms of nodal values of the examined primal cell. The balance equation of each node is built partially, calculating only the fluxes belonging to the considered cell.

With both methods the systems of linear equations defining the problem is built. Using the "*one node at time*" procedure the fundamental matrix is defined row by row. Adopting the "*one cell at time*" procedure a local system of linear equations is built involving the nodal values of the considered primal cell and the flux generated or absorbed in the dual parts of the primal volume associated to each primal node:

$$\mathbf{k}_c \mathbf{u}_c = \mathbf{S}_c. \tag{19}$$

These equations must be assembled in the global system considering the indices associated to the primal nodes in the global numbering adopted for the primal nodes. Even if the two methods are completely equivalent from the theoretical point of view, the "one cell at time" strategy results probably more convenient in a practical implementation of the method. Usually, for each primal cell is directly stored the list of the primal vertexes. The 'one cell at time" procedure is therefore straightforward available. On the other hand, detecting the set of primal cell sharing a primal nod can be computationally more expensive.

2.8 Convergence tests

In order to assess the numerical accuracy and the convergence rate of the presented implementation of the CM, numerical tests was performed solving the Laplace equation $\nabla^2 u(x,y,z) = 0$ over a simple geometry with Dirichlet boundary conditions. Two test functions were used:

$$T1(x,y,z) = e^x \sin y + e^y \sin z + e^z \sin x \tag{20}$$

and

$$T2(x,y,z) = e^z (\cos x + \cos y + \sin x + \sin y). \tag{21}$$

As reference domain a cube with unit edge was adopted: the cube was centred in the origin of the global Cartesian reference system and was aligned with the reference axes. Two kind of meshes were considered as primal cell complex: a generic

10-node tetrahedra mesh (Fig. 6), with no regularity in the spatial positioning of the nodes and a regular mesh composed by tetrahedra with uniform geometry over the volume (Fig. 7). For this second mesh a two step procedure has been adopted: a first second-order hexahedra mesh was been created to obtain a regular subdivision of the original volume with an imposed side size; each hexahedra was then be divided in tetrahedra. This procedure produces a mesh of tetrahedra characterized by high regularity which is referred in literature as uniform tetrahedralization [Hannukainen, Korotov, and Krizek (2009); Krizek (2005)].
The presented formulation for the CM using the quadratic tetrahedra as primal cells was implemented in a in-house Matlab/Octave code. A direct solver was used to solve the fundamental equation, limiting the numerical errors to the round off of the used machine.

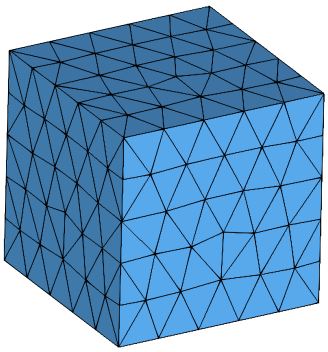

Figure 6: Generic mesh of 10-node tetrahedra.

As comparison, the same tests (using both the same meshes and the same boundary conditions) were replicated with the FEM using the Ansys commercial suite; to best replicate the conditions of the CM tests, the second-order tetrahedron constituted by the SOLID87 element was adopted and the sparse direct solver was selected to calculate the solution.
The accuracy of the numerical solution was assessed calculating the root mean square difference between the numerical solution and the exact solution of the problem, at internal nodes.
The root mean square error for the two tests is plotted against the edge length of the primal mesh in Fig. 8 for the generic mesh and Fig. 9 for the uniform mesh. The equation of the linear regression of the obtained values is also reported. The corresponding data are reported in Tab. 2 and Tab. 1.

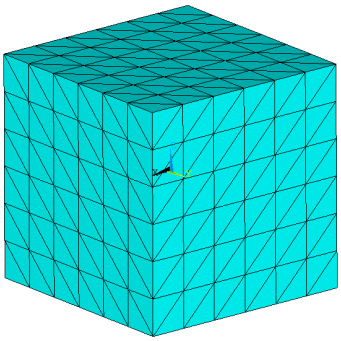

Figure 7: Mesh of 10-node tetrahedra obtained from a regular partitioning of the geometry.

Table 1: Convergence rate analysis: mean square difference between numerical results and theoretical values for the test functions Eq. 20 and Eq. 21 using a uniform tetrahedralization; both CM and FEM results are reported.

cell edge length	CM - mean square error		FEM - mean square error	
	function T1	function T2	function T1	function T2
0.33	5.60E-005	1.57E-004	4.16E-005	1.28E-004
0.25	1.63E-005	5.15E-005	1.40E-005	4.25E-005
0.20	7.99E-006	1.48E-005	5.89E-006	1.43E-005
0.17	3.11E-006	7.92E-006	2.72E-006	7.89E-006
0.14	1.74E-006	4.36E-006	1.51E-006	4.34E-006
0.13	1.40E-006	3.80E-006	1.07E-006	2.99E-006
0.11	8.42E-007	1.56E-006	5.94E-007	1.50E-006
0.10	4.68E-007	1.14E-006	4.20E-007	1.16E-006

Table 2: Convergence rate analysis: mean square difference between numerical results and theoretical values for the test functions Eq. 20 and Eq. 21 using a generic mesh; both CM and FEM results are reported.

cell edge length	**CM - mean square error**		**FEM - mean square error**	
	function T1	**function T2**	**function T1**	**function T2**
0.25	4.10733e-05	5.12121e-05	3.90999e-05	4.71238e-05
0.125	3.99E-006	5.04E-006	4.22414e-06	5.19181e-06
0.0625	3.72418e-07	4.82215e-07	4.06564e-07	5.10299e-07
0.03125	3.95E-008	5.44E-008	3.81627e-08	4.83266e-08

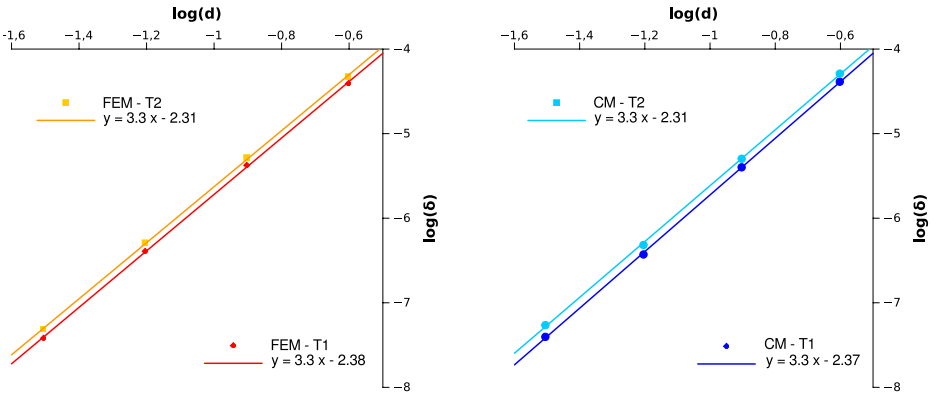

Figure 8: Convergence rate analysis: mean square difference (ε) versus cell edge length (d) for the test functions using the **generic mesh** of second order tetrahedra. The results obtained with the FEM are plotted on the left, those obtained using the CM are plotted on the right. The logarithmic scale is adopted.

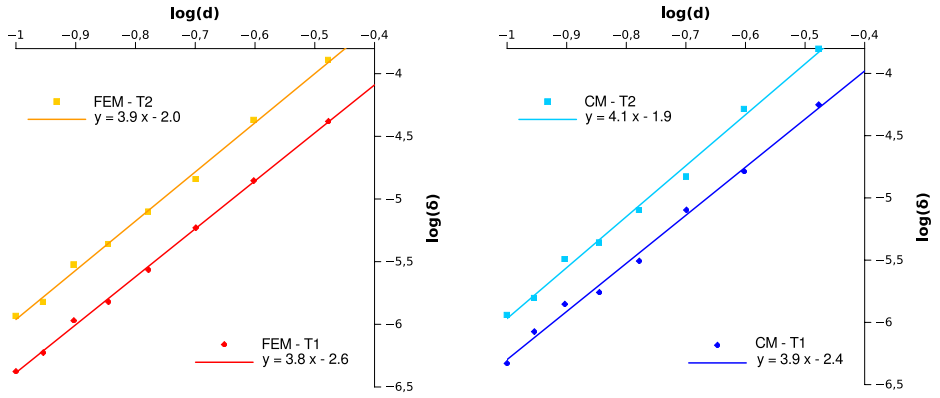

Figure 9: Convergence rate analysis: mean square difference (ε) versus cell edge length (d) for the test functions using the **uniform mesh** of second order tetrahedra. The results obtained with the FEM are ploted on the left, those obtained using the CM are plotted on the right. The logarithmic scale is adopted.

3 Conclusion

The Cell Method is a numerical method based in algebraic discrete formulation of physical law. It has been applied to many different fields, in both two and three dimensional problems. The quadratic formulation has been applied for the two dimensional problems in both harmonic problems (thermal conduction, [Tonti (2001b)]) and biharmonic problems (plane elasticity, [Cosmi (2001)]). Adopting the quadratic formulation, the 4th order of convergence has been reached in solving the Laplace equation over a uniform triangulation and basing the dual cells on the Gauss points of the primal edges. The comparison studies demonstrated that the CM is able to reach both a numerical accuracy and convergence rate comparable with that obtained by the FEM in solving the studied reference problems.

To date, for the three dimensional cases only the linear formulation has been presented.

In this paper the quadratic formulation to solve the Laplace equation in three dimensional domain has been presented. Adopting the 10-nodes tetrahedron as primal cell, the physical quantities involved in the balance equation have been described in their analytical expression.

Using the described formulation, a verification test relative to a simple domain has been presented to asses the accuracy as well as the convergence rate of the numerical solution obtained with the CM in solving the Dirichelet problem. Two different harmonic functions were adopted to impose the boundary conditions and two dif-

ferent kind of meshes (generic and uniform tetrahedralization) were used as primal complex.
As comparison, the results obtained with a commercial code implementing the FEM were considered. The FEM analyses were performed using as elements the primal cells defined for the CM approach. As for the CM, the numerical solution of the fundamental equation was obtained using a direct solver, in order to avoid differences due to convergence tolerances of an iterative algorithm.
The difference between numerical and theoretical solution of the Dirichlet problem at the internal nodes was considered. As accuracy metric the root mean square value of that difference has been adopted.
For both the harmonic functions used as test both the root mean square error and convergence rate of CM resulted comparable with that obtained using the FEM. Using the uniform tetrahedrlized mesh, the CM showed to be able, as well as the FEM, to obtain an order of convergence close to 4 for both the test functions. This convergence rate is greater than that usually achievable with the Finite Element Method. This behaviour is what is reported as superconvergence phenomenon [Krizek (2005)], and is mainly related to the high regularity of the used mesh decomposition, which is usually referred as uniform tetrahedralization [Krizek (2005)].
CM and FEM resulted comparable in terms of accuracy and convergence rate. It is worth to remember that, in in the present study, the homogeneous problem $\nabla^2 u = 0$ was considered. This fact did not involve the well known difference between the two methods in the discretisation of the source therm [Tonti (2002)]. In fact, when a distributed source is present, the source term resulted the same for CM and FEM. Nevertheless, concentrated sources are computed differently by the two methods: the CM assigns the whole concentrated sources to the primal node associated to the dual volume where the source is placed. The FEM distributes the source to the nodes of the element where the source is placed, following the "lever rule".
The presented results confirm the agreement between CM and the FEM even for quadratic tetrahedral elements. This provides another important confirmation of the consistency of the CM as a tool for the numerical solution of technical problems. Allowing the same accuracy of FEM, the CM adopts an approach that avoid the differential formulation, the concept of residual, and the orthogonality of the residual to the shape functions, the CM could constitute a reliable basis for approaching problems in that fields (e.g. biomechanics, fracture mechanics, ..) where the discrete nature of the studied problems could found a powerful agreement with the philosophy at the basis of the CM.

Acknowledgement: The author would like to thank Ing. Matteo Cataldi for the

valuable support.

References

Babuška, I.; Strouboulis, T.; Upadhyay, C.; Gangaraj, S. (1996): Computer-based proof of the existence of superconvergence points in the finite element method; superconvergence of the derivatives in finite element solutions of laplace's, poisson's, and the elasticity equations. *Numerical Methods for Partial Differential Equations*, vol. 12, no. 3, pp. 347–392.

Brunett, D. S. (1987): *Finite Element Analysis, from Concept to Applications*. Addison-Wesley.

Chen, L. (2006): Superconvergence of tetrahedral linear finite elements. *Int. J. Numer. Anal. Model*, vol. 3, no. 3, pp. 273–282.

Cosmi, F. (2001): Numerical solution of plane elasticity problems with the cell method. *Computer Methods in Engineering & Sciences, CMES*, vol. 2, no. 3.

Cosmi, F. (2005): Elastodynamics with the cell method. *Computer Modeling in Engineering & Sciences, (CMES)*, vol. 8, no. 3, pp. 191–200.

Cosmi, F. (2008): Dynamics analysis of mechanical components: a discrete model for damping. *CMES Computer Modeling in Engineering & Sciences, Tech Science Press, Irvine, CA, USA, ISSN*, pp. 1526–1492.

Cosmi, F.; Dreossi, D. (2007): Numerical and experimental structural analysis of trabecular architectures. *Meccanica*, vol. 42, no. 1, pp. 85–93.

Cosmi, F.; Hoglievina, M. (2010): An application of the cell method to multiaxial fatigue assessment of a test component under different criteria. *Strain*, vol. 46, no. 2, pp. 148–158.

Ferretti, E. (2003): Crack propagation modeling by remeshing using the cell method (cm). *CMES: Computer Modeling in Engineering & Sciences*, vol. 4, no. 1, pp. 51–72.

Ferretti, E. (2004a): Crack-path analysis for brittle and non-brittle cracks: A cell method approach. *CMES: Computer Modeling in Engineering & Sciences*, vol. 6, pp. 227–244.

Ferretti, E. (2004b): A cell method (cm) code for modeling the pullout test step-wise. *CMES: Computer Modeling in Engineering & Sciences*, vol. 6, no. 5, pp. 453–476.

Ferretti, E. (2005a): A local strictly nondecreasing material law for modeling softening and size-effect: a discrete approach. *CMES: Computer Modeling in Engineering & Sciences*, vol. 9, no. 1, pp. 19–48.

Ferretti, E. (2005b): On nonlocality and locality: Differential and discrete formulations. *ICF XI*, vol. 1, pp. l.

Ferretti, E. (2009): Cell method analysis of crack propagation in tensioned concrete plates. *CMES: Computer Modeling in Engineering & Sciences*, vol. 54, no. 3, pp. 253–282.

Ferretti, E. (2013a): A cell method stress analysis in thin floor tiles subjected to temperature variation. *CMC: Computers, Materials & Continua*, vol. 36, no. 3, pp. 293–322.

Ferretti, E. (2013b): The cell method: an enriched description of physics starting from the algebraic formulation. *CMC: Computers, Materials & Continua*, vol. 36, no. 1, pp. 49–72.

Ferretti, E.; Casadio, E.; Di Leo, A. (2008): Masonry walls under shear test: a cm modeling. *CMES: Computer Modeling in Engineering & Sciences*, vol. 30, no. 3, pp. 163–190.

Hannukainen, A.; Korotov, S.; Krizek, M. (2009): Nodal o(h4)-superconvergence in 3d by averaging piecewise linear, bilinear, and trilinear fe approximation. *Journal of Computational Mathematics*, vol. 28, no. 1, pp. 1–10.

Krizek, M. (1994): Superconvergence phenomena in the finite element method. *Computer Methods in Applied Mechanics and Engineering*, vol. 116, no. 1-4, pp. 157–163.

Krizek, M. (2005): Superconvergence phenomena on three-dimensional meshes. *International Journal of Numerical Analysis and Modeling*, vol. 2, no. 1, pp. 43–56.

Lin, R.; Zhang, Z. (2008): Natural superconvergence points in three-dimensional finite elements. *SIAM J. Numer. Anal.*, vol. 46, no. 3, pp. 1281–1297.

Marrone, M. (2001): Computational aspects of the cell method in electrodynamics - abstract. *Journal of Electromagnetic Waves and Applications*, vol. 15, pp. 407–408(2).

Taddei, F.; Pani, M.; Zovatto, L.; Tonti, E.; Viceconti, M. (2008): A new meshless approach for subject-specific strain prediction in long bones: Evaluation of accuracy. *Clinical biomechanics (Bristol, Avon)*, vol. 23, no. 9, pp. 1192–9.

Tonti, E. (2001a): A direct discrete formulation for the wave equation. *Journal of Computational Acoustics*, vol. 9, no. 4, pp. 1355–1382.

Tonti, E. (2001b): A direct discrete formulation of field laws: The cell method. *CMES: Computer Modeling in Engineering & Sciences*, vol. 2, no. 2, pp. 237–258.

Tonti, E. (2002): Finite formulation of electromagnetic field. *IEEE Transactions on Magnetics*, vol. 38, no. 2(I), pp. 333 – 336.

Tonti, E.; Zarantonello, F. (2009): Algebraic formulation of elastostatics: the cell method. *CMES: Computer Modeling in Engineering & Sciences*, vol. 39, no. 3, pp. 201–236.

Tonti, E.; Zarantonello, F. (2010): Algebraic formulation of elastodynamics: the cell method. *CMES: Computer Modeling in Engineering & Sciences*, vol. 64, no. 1, pp. 37–70.

Zhang, Z.; Lin, R. (2005): Locating natural superconvergent points of finite element methods in 3d. *Internat J Numer Anal Model*, vol. 2, no. 1, pp. 19–30.

Zienkiewicz, O. C.; Taylor, R. L. (1989): *The Finite Element Method - Basic Concepts and Linear Applications*, volume 1. McGraw-Hill - London, iv edition.

Zovatto, L.; Nicolini, M. (2003): The meshless approach for the cell method: a new way for the numerical solution of discrete conservation laws. *International Journal of Computational Engineering Science*, vol. 4, pp. 869–880.

Zovatto, L.; Nicolini, M. (2006): Extension of the meshless approach for the cell method to three-dimensional numerical integration of discrete conservation laws. *International Journal for Computational Methods in Engineering Science and Mechanics*, vol. 7, no. 2, pp. 69–79(11).

Zovatto, L.; Nicolini, M. (2007): Improving the convergence order of the meshless approach for the cell method for numerical integration of discrete conservation laws. *International Journal for Computational Methods in Engineering Science and Mechanics*, vol. 8, no. 5, pp. 273 – 281.

Appendix A: Local coordinates of the points that define the dual surfaces

A significant advantage of using the local affine coordinates is the possibility to deal with a regular geometry independently from the actual geometry of the primal cell. Particularly, that is useful to collocate the points which define the surfaces bounding the dual volumes onto each primal cell.
The local affine coordinates of the vertexes of the cell are reported in Tab. 3. Tab. 4 reports the local coordinates of the barycentre of the cell and of its surfaces.

Local coordinates of the points used to define the dual surfaces following the procedure presented in section 2.1 are reported in Tab. 6, Tab. 7 and Tab. 8. The notation reported in Fig. 2 and Fig. 3 is adopted. A parametric form is adopted: using the Gauss points of the primal edges, these parameters are worth $\alpha = 1/\left(2\sqrt{3}\right)$ and $\beta = 1 - \alpha$.

Table 3: local affine coordinates of the primal nodes

	Primal node									
	h	***i***	***j***	***k***	***m***	***n***	***o***	***p***	***q***	***r***
ξ	0	1	0	0	1/2	1/2	0	0	1/2	0
η	0	0	1	0	0	1/2	1/2	0	0	1/2
ζ	0	0	0	1	0	0	0	1/2	1/2	1/2

Table 4: local affine coordinates of the baricentre of the cell and of its surfaces

	Barycentre				
	g	g_h	g_i	g_j	g_k
ξ	1/4	1/3	0	1/3	1/3
η	1/4	1/3	1/3	0	1/3
ζ	1/4	1/3	1/3	1/3	0

Table 5: local affine coordinates of the dual points close to the primal vertex h

	Dual nodes						
	h_1	h_2	h_3	h_{12}	h_{23}	h_{31}	h_g
ξ	α	0	0	$\alpha/2$	0	$\alpha/2$	$\alpha/3$
η	0	α	0	$\alpha/2$	$\alpha/2$	0	$\alpha/3$
ζ	0	0	α	0	$\alpha/2$	$\alpha/2$	$\alpha/3$

Table 6: local affine coordinates of the dual points close to the primal vertex i

	Dual nodes						
	i_1	i_2	i_3	i_{12}	i_{23}	i_{31}	i_g
ξ	β	β	β	β	β	β	β
η	α	0	0	$\alpha/2$	0	$\alpha/2$	$\alpha/3$
ζ	0	0	α	0	$\alpha/2$	$\alpha/2$	$\alpha/3$

Table 7: local affine coordinates of the dual points close to the primal vertex j

	Dual nodes						
	j_1	j_2	j_3	j_{12}	j_{23}	j_{31}	j_g
ξ	0	α	$\alpha/2$	$\alpha/2$	$3\alpha/4$	$\alpha/4$	$\alpha/2$
η	β	β	β	β	β	β	β
ζ	0	0	α	0	$\alpha/2$	$\alpha/2$	$\alpha/3$

Table 8: local affine coordinates of the dual points close to the primal vertex k

	Dual nodes						
	k_1	k_2	k_3	k_{12}	k_{23}	k_{31}	k_g
ξ	0	α	0	$\alpha/2$	0	$\alpha/2$	$\alpha/3$
η	0	0	α	0	$\alpha/2$	$\alpha/2$	$\alpha/3$
ζ	β	β	β	β	β	β	β